

## Chapter 6: Photolabile structure-directing agents for zeolite synthesis

### Abstract

The synthesis, photocleavage, and structure-directing ability of the photolabile molecule 8,8-dimethyl-2-(2-nitrophenyl)-1,4-dioxo-8-azoniaspiro[4.5]decane hydroxide (P-SDA 1) is presented and discussed. The organic molecule is synthesized via ketalization procedures, followed by amine quaternization and ion exchange to the final hydroxide form, generating P-SDA 1 in approximately 50% overall yield. Photolytic cleavage of the molecule proceeds via long-wave UV radiation with a Hg arc lamp to generate the unstable 2-nitrosophenylcarbonyl derivative of the 2-nitrophenylethylene glycol photochemical protecting group and 1,1-dimethyl-4-oxopiperidium hydroxide. Cleavage of the photolytic P-SDA 1 is demonstrated in a homogeneous solution of acetonitrile, and intercalated into a dealuminated zeolite FAU, an open-framework zeolite. Attempts to synthesize silicate and aluminosilicate zeolites through procedures similar to those used to prepare various compositions of the BEA\* and MFI zeolite structures, using P-SDA 1 as the structure-directing agent, resulted in the formation of primarily amorphous and layered materials. One synthesis did yield crystalline material with the MFI zeolite topology; however, this synthetic result was not reproducible.

### 1. Introduction

As more zeolite phases are discovered through the use of novel and expensive organic structure-directing agents, and used in non-traditional applications like electronic devices and chemical sensors, the need for a low-cost alternative to the standard calcination process, which destroys the organic molecules, increases. Previous work by Lee et al.

demonstrated a combustion-free zeolite synthesis method that removes structure-directing agents (SDAs) from pores, by using various acid-cleavable ketal compounds that contain quaternary ammonium cations.<sup>1,2</sup> The acid-cleavable ketal compounds can be cleaved into smaller ketone- and diol-functionalized fragments, which can then be recombined into the original molecule for further zeolite syntheses. This method avoids problems commonly caused by high-temperature calcination, such as crack formation in zeolite thin films or membranes due to thermal stresses within the film and at the film / substrate interface.<sup>3</sup> However, this method may not be suitable for nanoparticle suspensions, thin films, or for many zeolite phases in general due to the nature of the extraction process – i.e., the presence of acid and water may change the suspension properties and can cause hydrolysis of unstable zeolite phases due to their siliceous nature, and like calcination, can cause aggregation of zeolite nanoparticle colloids due to Si-O-Si bridging.<sup>4</sup> Therefore, an alternative to calcination that is both simple and more compatible with end-use processing and fabrication steps for non-traditional zeolite applications would be valuable.

The use of UV radiation, as opposed to aqueous acid, to cleave the structure-directing agents would provide a simpler method of liberating the zeolite pores. Additionally, it could decrease the likelihood of film defect formation due to high temperature calcination in zeolite thin films and membranes, and could reduce aggregation in colloidal suspensions, thus avoiding complicated methods for reducing aggregation during template removal. These methods include the use of organic or polymeric matrices to physically bar aggregation<sup>5</sup>, the surface functionalization of colloidal particles to

minimize interactions<sup>6</sup>, and acid extraction of structure-directing agents from surface-modified zeolite nanoparticles.<sup>7</sup> Photolysis of the structure-directing agent could therefore be a useful strategy for a variety of applications developed using colloidal zeolite suspensions and zeolite nanoparticles, such as thin films and membranes (through spin / dip coating)<sup>8</sup>, macroscopic, ordered zeolite structures (through macropatterning or macrotemplating)<sup>9</sup>, micro-/mesoporous materials (through seeding)<sup>10</sup>, medical diagnostics (through incorporation of Gd<sup>3+</sup> ions for magnetic resonance imaging)<sup>11</sup>, and chemical sensors<sup>12</sup>, due to its relatively simple strategy compared with other techniques to minimize aggregation.

Towards this end, the development of partially recyclable, photo-cleavable structure-directing agents, is proposed, wherein the structure-directing agent is disassembled through photolysis within the zeolite pore space, removed, and then reassembled for the manufacture of additional zeolites – without the complete destruction of either the organic structure-directing agent or damage to the inorganic zeolite framework. The initial photolabile structure-directing agent to be developed is a derivative of 8,8-dimethyl-2-phenyl-1,4-dioxo-8-azoniaspiro[4,5]decane hydroxide, an acid-cleavable molecule that has been demonstrated to produce the zeolite known as mordenite (structure code MOR). This new molecule is a member of the 2-nitrobenzyl class of photochemical protecting groups commonly used in the organic synthesis of polyfunctional molecules (Figure 6.1b).<sup>2,13</sup> Here, its synthesis and photolysis is presented, and its feasibility as a structure-directing agent for common silicate and aluminosilicate zeolites is evaluated.

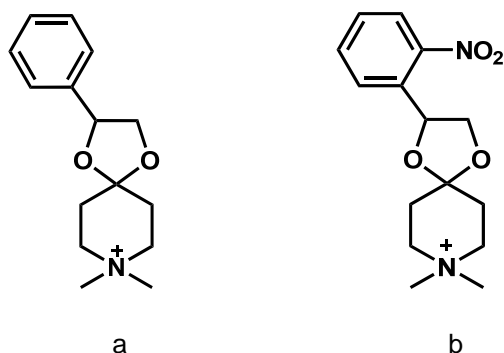


**Figure 6.1** (a) Acid-cleavable structure-directing agent 8,8-dimethyl-2-phenyl-1,4-dioxaspiro[4,5]decane hydroxide; (b) potential photolabile structure-directing agent, 8,8-dimethyl-2-(2-nitrophenyl)-1,4-dioxaspiro[4,5]decane hydroxide

## 2. Results and Discussion

### 2.1 P-SDA 1 Synthesis

Although there are no reports in the literature of the synthesis of P-SDA 1, its preparation may be envisioned by the use of standard ketalization reaction techniques, followed by quaternization of the secondary amine, and finally, ion exchange of its iodide counter-ion to the hydroxide form (Figure 6.2).<sup>14,15</sup> Since the product molecule (P-SDA 1) may be cleaved by both acids as well as long-wave UV radiation, the initial ketalization reaction is run under an inert atmosphere in a covered apparatus, and is neutralized upon reaction completion by the addition of a small amount of a saturated solution of sodium bicarbonate in water while stirring the reaction mixture. Ketalization reactions of this type generally proceed to completion only if the water generated during the ring-formation is removed, hence a Dean-Stark apparatus is used during reflux. Although

standard literature procedures for ketalization reactions suggest that the diol be in excess of the ketone (to protect the ketone)<sup>13</sup>, the diol in this case, 1-(2-nitrophenyl)ethane-1,2-diol (Aldrich), is very expensive<sup>1</sup> and is therefore used as the limiting reagent. The ketone (4-piperidone HCl•H<sub>2</sub>O, Fluka) to diol molar ratio is at least 3:1. Crude <sup>1</sup>H nuclear magnetic resonance (NMR) spectroscopy data for this molecule before amine quaternization indicates peaks at 2.1, 3.1, 3.8, 4.6, 5.6, 7.6, 7.8, 8.1, and 8.3, in addition to low-intensity peaks due to the presence of small amounts of impurities at 1.0, 2.3, 3.4, 5.1, 7.5, and 7.7.

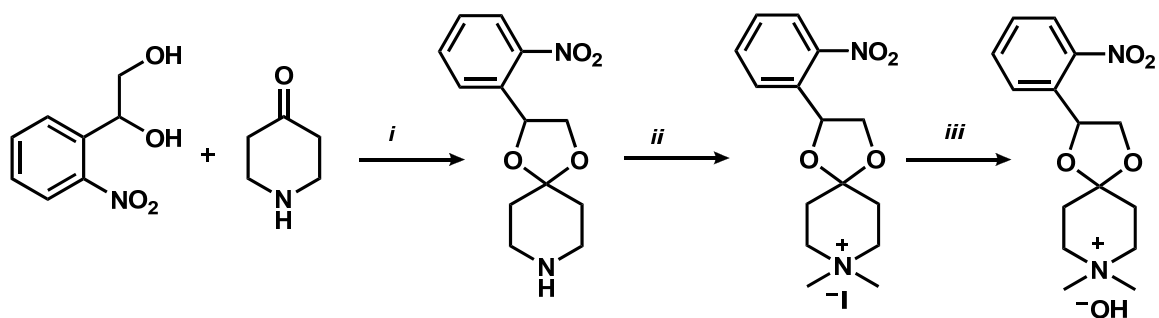


**Figure 6.2** Proposed synthetic route for the preparation of P-SDA 1: (i) ketalization reaction; (ii) quaternization of the secondary amine; (iii) ion exchange of the quaternary amine counter-ion

To purify the ketal product, which is a reddish-colored resin, water / chloroform extraction was used to separate the excess ketone from the product ketal. Further

<sup>1</sup> approximately \$325 for five grams

purification of the product by solid-liquid chromatography on a silica gel 60 column was attempted, but resulted in the breakdown of the molecule due to the slightly acidic nature of the silica gel. Purification by recrystallization was then attempted with a large variety of solvent systems, with varying degrees of success. A mixture of dichloromethane / hexanes appeared to yield the best results, although the product precipitated out of the solution as an oily substance, and not as a solid powder, as expected. Alternatively, repeated extraction from a water / chloroform solvent system resulted in adequate purification.

The amine quaternization reaction was tested in methanol for a variety of solution concentrations and molar equivalents of methyl iodide. The reaction was run under an inert atmosphere shielded from light sources, as previously discussed, and the methyl iodide to amine ratio was at least 5 : 1 to reduce the reaction time. Lower amounts of methyl iodide could be used, but this caused the reaction time to extend to several days to produce a quaternized product in over 40 % yield. Upon reaction completion, the product was recovered, and recrystallized from chloroform and ether. The ketal's iodide counter-ion was then ion-exchanged with the hydroxide ion, and the extent of conversion was determined by acid titration. The resulting photo-cleavable structure-directing agent was then characterized by  $^1\text{H}$  NMR, as shown in Figure 6.3.

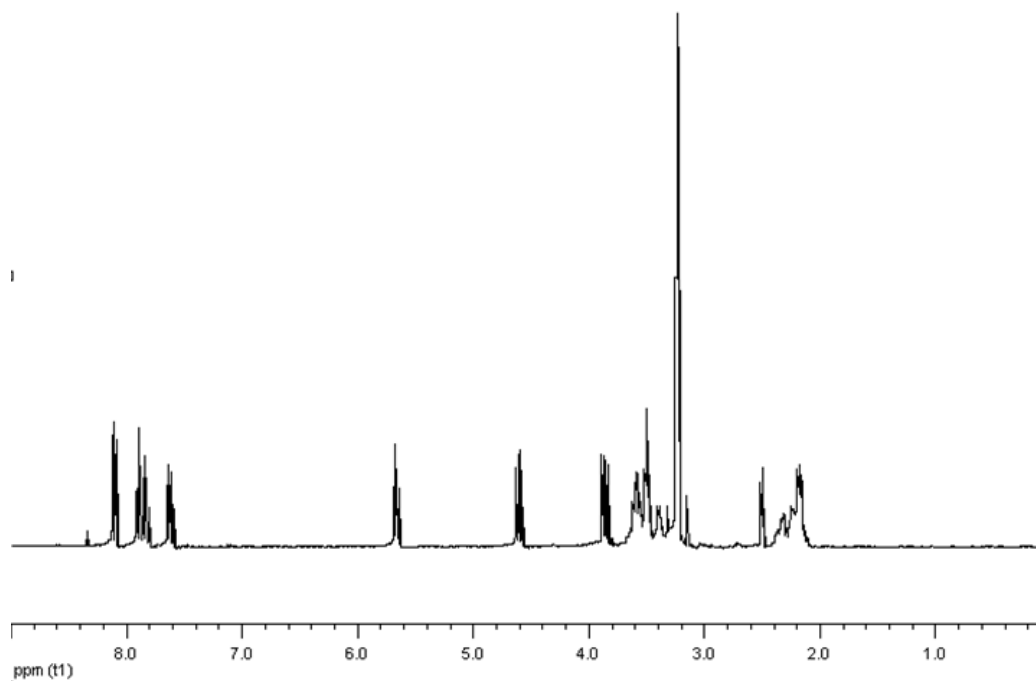


**Figure 6.3**  $^1\text{H}$  NMR spectrum of P-SDA 1 in its iodide salt form

The molecule was tested for thermal stability using thermogravimetric analysis (TGA) in its iodide salt form, which indicated that it experiences an initial mass loss of approximately 20% beginning at approximately 250 °C. This suggested that zeolite synthesis temperatures beyond this point will result in the breakdown of P-SDA 1 (Figure 6.4). Beyond 300 °C, another gradual mass loss occurred, but not all of P-SDA 1 was combusted off the sample pan at the end of the run; indeed, a small percent remained as black “coke” on the pan after the experiment finished. This type of coking can occur when aromatics are present in the sample. Also, the small endotherm at 200 °C is most likely a melting point for the sample. These data imply that the photolabile molecule is stable in the standard range of zeolite synthesis temperatures (although the stability of the molecule in caustic zeolite gels may differ from the given thermal stability).

Additionally, it was found that the iodide salt form of the ketal (the form obtained after step *ii* in Figure 6.2) is very stable to both air and visible light, whereas the photolabile molecule in its aqueous, ion-exchanged hydroxide form rapidly deteriorates when stored, unprotected to visible light, due to a combination of the effects of water and light on the ketal bond. Therefore, P-SDA 1 must be stored long-term in the iodide salt form and ion-exchanged just prior to use.

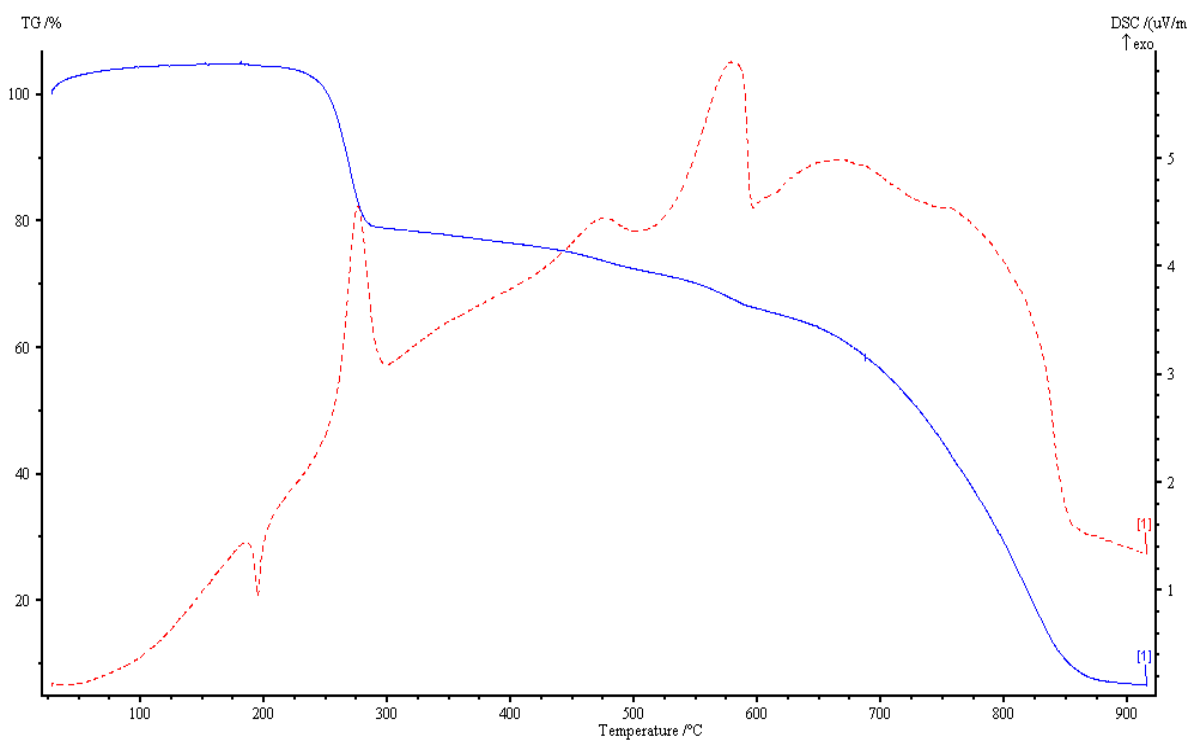


**Figure 6.4** TGA data of P-SDA 1 prior to conversion of quaternary ammonium iodide salt form to quaternary ammonium hydroxide material

## 2.2 Photolysis of P-SDA 1

As with all members of the 2-nitrobenzyl group of photoactive molecules, P-SDA 1 cleaves with long-wave UV radiation through a hydrogen-abstraction mechanism (Figure 6.5). P-SDA 1, however, has not been reported in the literature; therefore, the molecule's photolytic ability must be confirmed. To do this, the ketal in its iodide salt form was dissolved in a variety of solvents (acetonitrile, N,N-dimethylformamide, dimethylsulfoxide, water, benzene) and subjected to UV radiation with a wavelength of greater than 320 nm for various times following standard photo-cleavage procedures.<sup>13,15,16</sup> Unsurprisingly, it was found that protic solvents interfere with the cleavage of this molecule. Aprotic solvents, such as acetonitrile, however, allowed the complete cleavage of P-SDA 1 in its iodide salt form by irradiation after only one hour. The iodide salt form of the ketal was used in this case because the hydroxide form, when irradiated, completely decomposed due to the necessity of heavily concentrating the solution in order to follow standard photo-cleavage procedures, which led to the extremely basic solution destroying the molecule. The cleavage was followed using electrospray ionization mass spectroscopy (ESI MassSpec), which indicated the presence of the ketone cleavage fragment  $[M^+] = 128.08$  and did not detect the intact ketal  $[M^+] = 293.07$  after one hour.

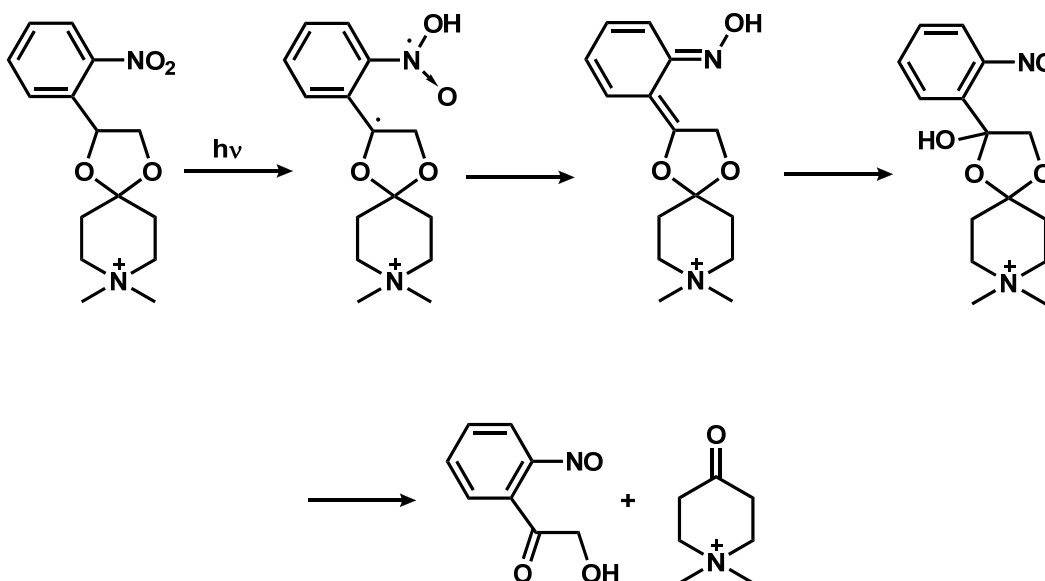


**Figure 6.5** Photolysis mechanism of P-SDA 1, generating 2-hydroxy-1-(2-nitrosophenyl)ethanone and 1,1-dimethyl-4-oxopiperidinium

However, the cleavage of P-SDA 1 in a homogeneous solution does not serve as a perfect test of its ability to cleave within a zeolite framework, which is its final destination.<sup>16</sup> To determine the effectiveness of cleaving within a cage, and to find and to eliminate potential problems that may arise during cleavage, the ketal was then intercalated into a large cage, pure-silica zeolite (trade-name Tosoh 390-HUA, structure code FAU) donated by Chevron. Standard intercalation procedures called for activating 300 mg of this zeolite with heat and vacuum for 12 hours, then injecting a solution of 20 mg of the ketal iodide salt in 0.8 mL acetonitrile and stirring the solution for 24 hours. Solid-state  $^{13}\text{C}$  cross-polarization magic-angle spinning nuclear magnetic resonance (CPMAS NMR, Figure 6.6) and TGA (Figure 6.7) were carried out on both the solid ketal (prior to

intercalation) and the zeolite sample (post-intercalation) to determine the success of the procedure. TGA data indicated that the zeolite was loaded with 16 wt % organic, and showed that the organic in the zeolite sample had the same characteristic curve as the pure iodide salt ketal.  $^{13}\text{C}$  CPMAS NMR indicated peaks for the pure iodide salt ketal at 148.0, 140.5, 134.7, 130.1, 124.4, 123.3, 104.1, 74.3, 69.5, 60.2, 52.3, 42.9, 30.5, and 25.2. The corresponding crude spectrum for the loaded zeolite sample showed broad peaks whose width incorporated the 148.0 – 123.3 ppm peaks and the 74.3 – 25.2 peaks. A smaller peak corresponding to the ketal carbon at 104.1 ppm was also present.

Initial attempts to cleave the adsorbed molecule failed due to the use of procedures better suited to homogeneous solutions than molecules adsorbed within the zeolite cage (Figure 6.6c). If cleaved, the  $^{13}\text{C}$  CPMAS NMR data would show a small peak at 200 ppm, due to the presence of a ketone. A modified procedure was then utilized. The new procedure called for the sample to be drop-coated in a thin layer onto glass slides, then irradiated. After photocleavage, the sample was scraped off the slides, and the P-SDA 1 fragments were extracted from the pore space using acetonitrile. The photocleavage was followed using infrared spectroscopy (IR), and yielded cleavage of the P-SDA 1 present in the zeolite material (Figure 6.8). This was demonstrated by the formation of the ketone carbon peak at  $1790\text{ cm}^{-1}$ . In this case, IR was used to follow the photolysis rather than  $^{13}\text{C}$  CPMAS NMR due to the very long experiment time required to obtain a good signal-to-noise ratio for this NMR spectrum.

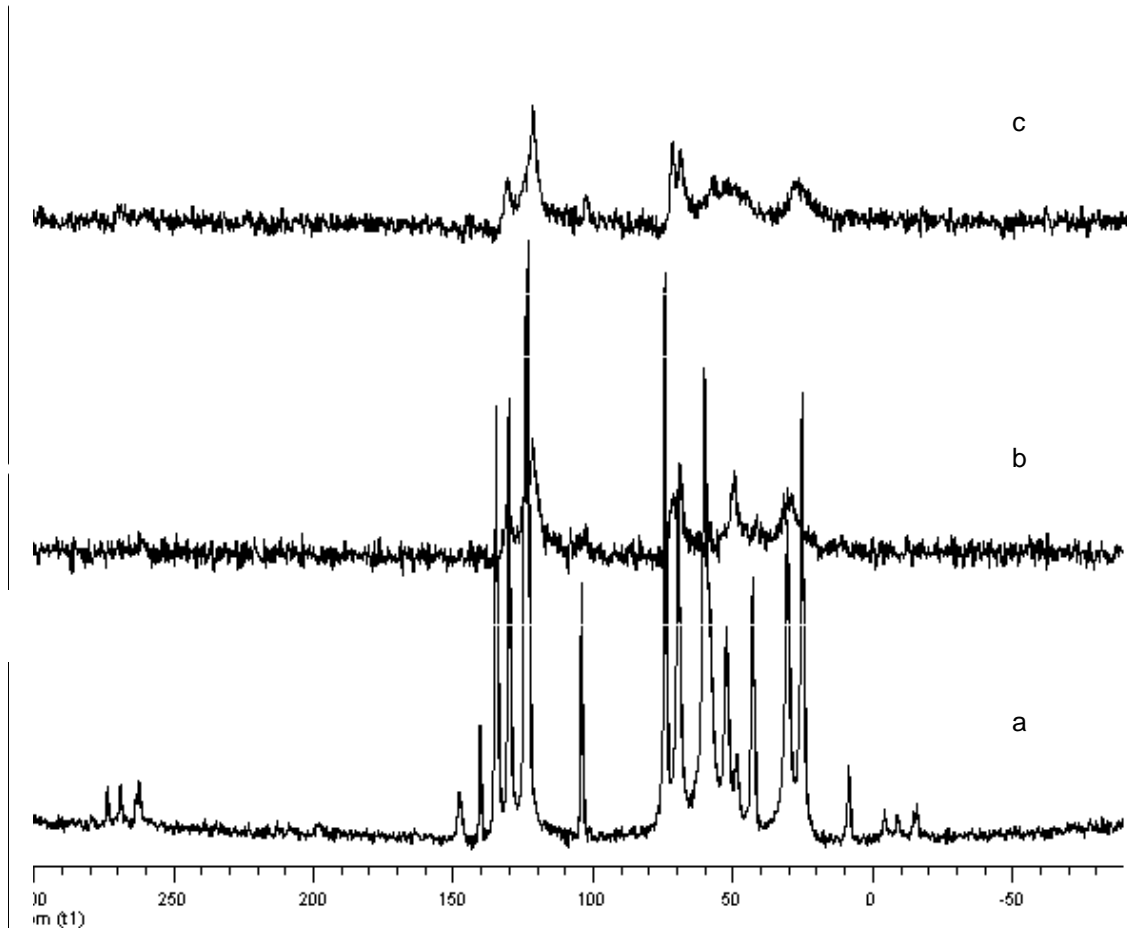


**Figure 6.6**  $^{13}\text{C}$  CPMAS NMR spectra of: (a) P-SDA 1 in the iodide salt form; (b) P-SDA 1 intercalated into the pure-silica zeolite with the FAU structure; (c) results of initial attempts to photocleave P-SDA 1 intercalated into the pure-silica FAU material demonstrate that cleavage did not occur, as the NMR data did not change

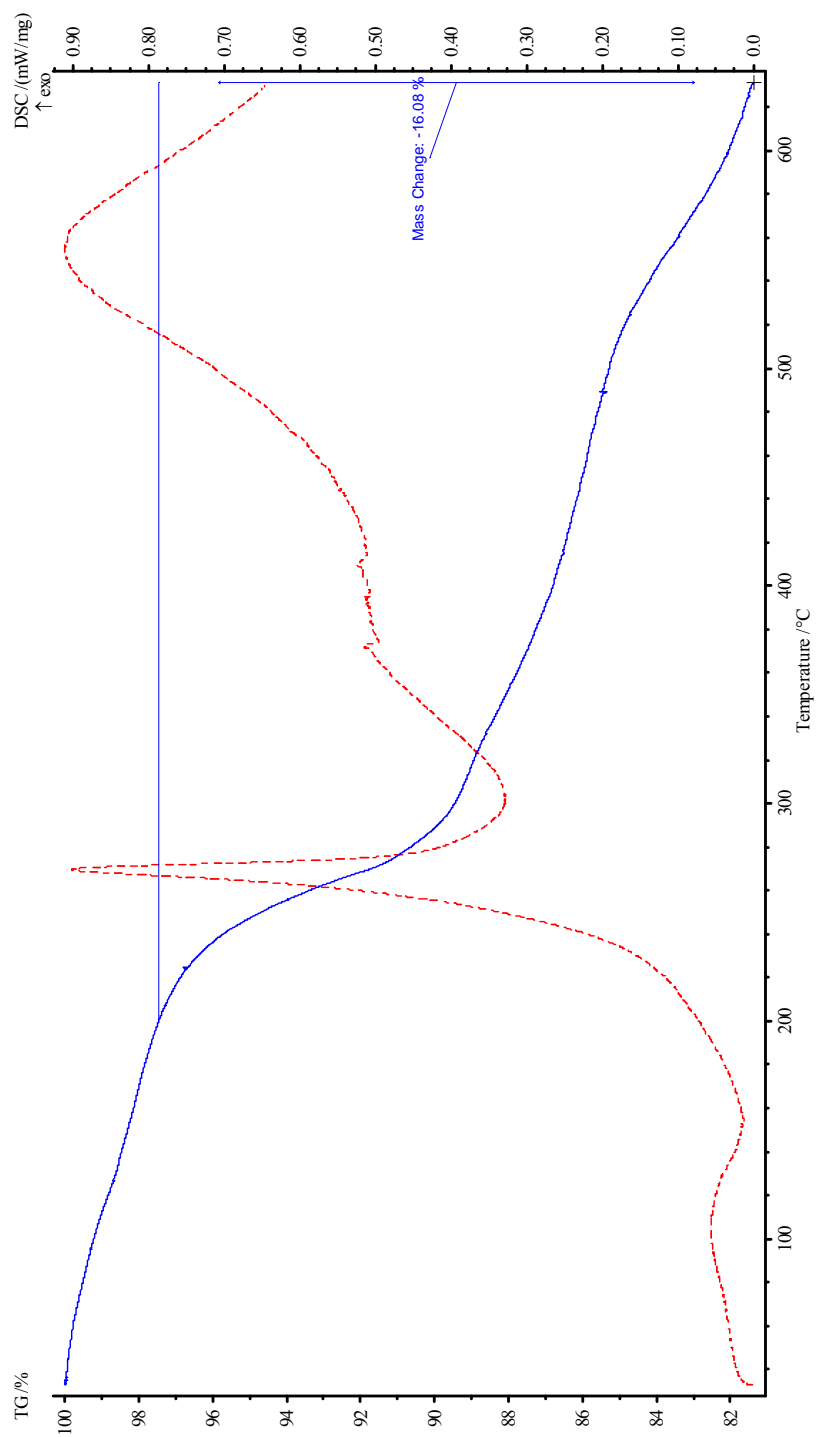


**Figure 6.7** TGA data of P-SDA 1 intercalated in pure-silica zeolite FAU

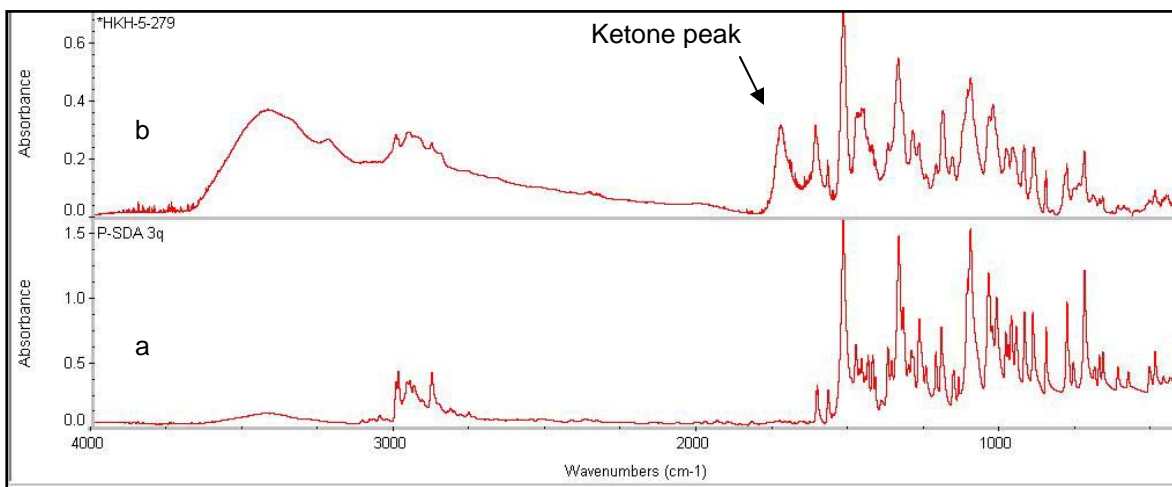


**Figure 6.8** IR spectra of (a) P-SDA 1; (b) P-SDA 1 subjected to photolysis while intercalated in pure-silica zeolite FAU

### 2.3 Zeolite Synthesis Using P-SDA 1

Initial attempts to crystallize zeolite materials using P-SDA 1 were based on synthetic procedures that formed the zeolite MOR using the acid-cleavable equivalent molecule in Figure 6.1a. Unfortunately, these syntheses produced amorphous materials, even at extremely long crystallization times. It is likely that the addition of the nitro group to the molecule adversely affected zeolite nucleation, perhaps due to the slight change in electrostatic interactions caused by the electron-withdrawing nitro group on the aromatic portion of the molecule. Docking calculations that evaluate the stability of the ketal within a zeolite structure based on van der Waals interactions between the guest molecule and the zeolite host were performed by A. Burton at Chevron, to determine if another zeolite could be a more appropriate host. These simulations suggested that the zeolite beta (BEA\*) would be an appropriate host for the photolabile molecule, given the

favorable stabilization energy of  $-12.0$  kJ / mol of P-SDA 1, thus making it likely that the ketal could form BEA\* given the correct synthesis conditions. The fit of the photolabile molecule inside the BEA\* framework is shown in Figure 6.9.

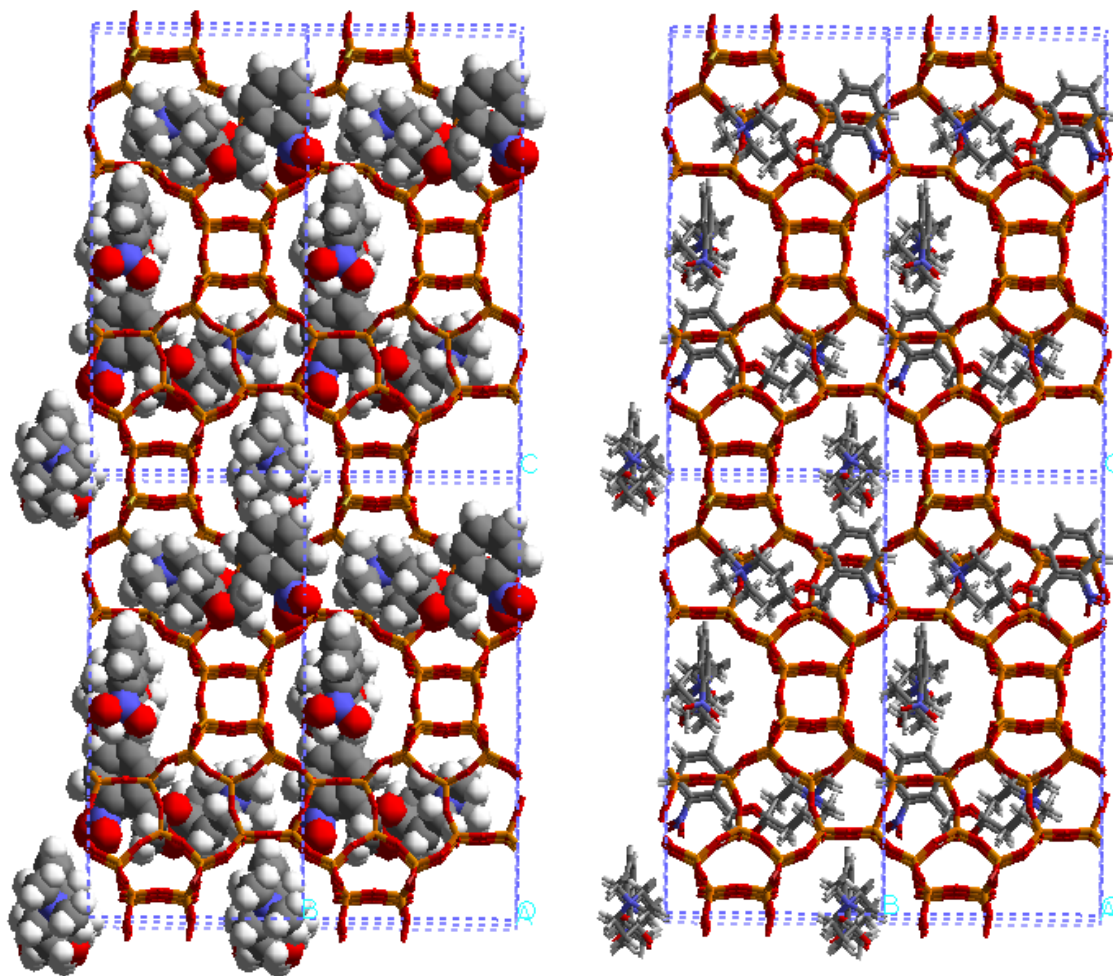


**Figure 6.9** Schematic representation of P-SDA 1 in zeolite BEA\* (docking calculations performed by A. Burton at Chevron)

Initial zeolite syntheses using P-SDA 1 as the structure-directing agent centered on standard aluminosilicate BEA\*, and borosilicate BEA\* (B-BEA\*) syntheses. Table 6.1 shows the various reaction conditions attempted and their results. Interestingly, BEA\* was never obtained, but a few of the BEA\* recipes yielded small zeolite MFI crystals, as indicated by the low intensity of the diffraction patterns. This initiated a switch to the zeolite MFI family of recipes, to determine if this structure would more easily form using procedures specific to this material. The zeolite phase MFI is known to crystallize over a wide range of conditions with many different structure-directing agents; in some cases, it has been known to form without a structure-directing agent.<sup>1,17,18,19,20,21</sup> MFI-based syntheses, then, could be an excellent model system to demonstrate the structure-directing capabilities of P-SDA 1. Generally, the MFI recipes were based on silicalite (pure-silica zeolite with the MFI structure) recipes, and yielded the layered phase kanemite (due to high sodium content) as well as small MFI crystals. A seeded silicalite recipe using calcined silicalite seeds, however, resulted in a more crystalline sample with a larger crystal size, and a definite MFI structure. In these materials, <sup>13</sup>C CPMAS NMR spectra (Figure 6.10) showed that the occluded organics did not include a ketone-containing fragment of the P-SDA 1 molecule (represented by a peak at 200 ppm), showing that the organic was intact. The peaks in this data set were quite broad due to interactions with the inorganic species. Overall, however, this synthesis was found to be irreproducible after several attempts to repeat it.

**Table 6.1** Synthesis conditions for zeolite synthesis using P-SDA 1 as the structure-directing agent

Recipe	Seed	Gel Composition	t, days	T, °C	Stir	Results
B-BEA	No	0.017 Na <sub>2</sub> B <sub>4</sub> O <sub>7</sub> *10H <sub>2</sub> O / 1 SiO <sub>2</sub> / 0.56 SDA / 23 H <sub>2</sub> O	7	150	No	Amorphous
	No	0.034 Na <sub>2</sub> B <sub>4</sub> O <sub>7</sub> *10H <sub>2</sub> O / 1 SiO <sub>2</sub> / 0.56 SDA / 23 H <sub>2</sub> O	7	150	No	Amorphous
	No	0.0039 Na <sub>2</sub> B <sub>4</sub> O <sub>7</sub> *10H <sub>2</sub> O / 1 SiO <sub>2</sub> / 0.074 SDA / 5.15 H <sub>2</sub> O	15	150	No	MFI (low intensity)
BEA	No	60 SiO <sub>2</sub> / Al <sub>2</sub> O <sub>3</sub> / 11 NaOH / 30 SDA / 1500 H <sub>2</sub> O	4	165	No	Amorphous
	No	60 SiO <sub>2</sub> / Al <sub>2</sub> O <sub>3</sub> / 11 NaOH / 30 SDA / 1500 H <sub>2</sub> O	15	165	No	Amorphous
	No	60 SiO <sub>2</sub> / Al <sub>2</sub> O <sub>3</sub> / 11 NaOH / 30 SDA / 1500 H <sub>2</sub> O	12	165	Yes	MFI (low intensity)
	No	60 SiO <sub>2</sub> / Al <sub>2</sub> O <sub>3</sub> / 11 NaOH / 30 SDA / 1500 H <sub>2</sub> O	15	165	Yes	Amorphous
	No	60 SiO <sub>2</sub> / Al <sub>2</sub> O <sub>3</sub> / 11 NaOH / 30 SDA / 1500 H <sub>2</sub> O	15	165	Yes	Amorphous
	No	60 SiO <sub>2</sub> / Al <sub>2</sub> O <sub>3</sub> / 11 NaOH / 30 SDA / 1500 H <sub>2</sub> O	15	165	Yes	MFI
	No	60 SiO <sub>2</sub> / Al <sub>2</sub> O <sub>3</sub> / 11 NaOH / 30 SDA / 1500 H <sub>2</sub> O	15	165	Yes	Amorphous
	Yes	60 SiO <sub>2</sub> / Al <sub>2</sub> O <sub>3</sub> / 11 NaOH / 30 SDA / 1500 H <sub>2</sub> O	15	165	Yes	MFI (low intensity)
	Yes	60 SiO <sub>2</sub> / Al <sub>2</sub> O <sub>3</sub> / 11 NaOH / 30 SDA / 1500 H <sub>2</sub> O	15	165	Yes	Amorphous
PSZ MFI	Yes	20 SiO <sub>2</sub> / 2 Na <sub>2</sub> O / 2 SDA / 500 H <sub>2</sub> O	20	150	No	Kanemite
	Yes	20 SiO <sub>2</sub> / 2 Na <sub>2</sub> O / 2 SDA / 500 H <sub>2</sub> O	20	150	No	MFI / Kanemite
	Yes	20 SiO <sub>2</sub> / 1 Na <sub>2</sub> O / 2 SDA / 500 H <sub>2</sub> O	15	150	No	MFI
	Yes	20 SiO <sub>2</sub> / 1.5 Na <sub>2</sub> O / 2 SDA / 500 H <sub>2</sub> O	15	150	No	MFI / Kanemite
	Yes	20 SiO <sub>2</sub> / 1 Na <sub>2</sub> O / 2 SDA / 500 H <sub>2</sub> O	15	150	No	Amorphous
	Yes	20 SiO <sub>2</sub> / 1 Na <sub>2</sub> O / 2 SDA / 500 H <sub>2</sub> O	15	150	No	Kanemite

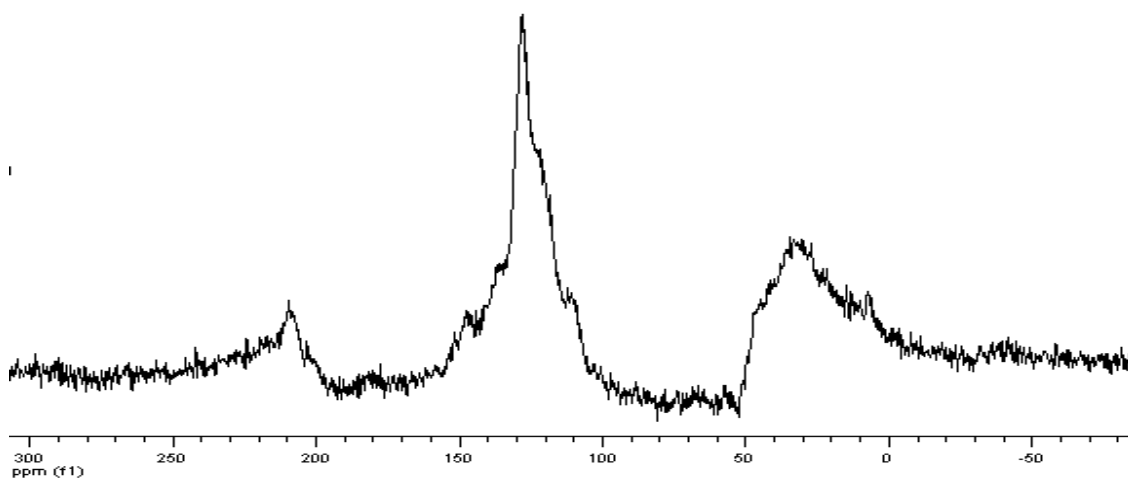


**Figure 6.10**  $^{13}\text{C}$  CPMAS NMR spectrum of P-SDA 1 in materials containing MFI crystals shows the molecule is still intact

After numerous attempts to reproducibly crystallize a zeolite material with a variety of synthetic conditions, it became apparent that the P-SDA 1 molecule, although capable of cleavage inside a large-cage zeolite, was inappropriate for use as a structure-directing agent under the conditions studied, despite the ability of its acid-cleavable counterpart to aid in the crystallization of MOR. This poor structure-directing ability could be due to many factors; among them could be, relative to its acid-cleavable counterpart, a change in the electrostatic interaction potential with the inorganic species due to the electron-withdrawing nature of the ring, a lower thermochemical stability in a zeolite gel at elevated temperatures compared, or the added bulk of the nitro group on the aromatic portion. Alternatively, the correct synthetic conditions for zeolite synthesis with this molecule may not have been evaluated. Although a combination of these is likely, it is

the last which may be the main culprit. The docking calculations of P-SDA 1 in zeolite BEA\* indicate that the molecule has a rather tight fit in the pore structure, which may prevent formation of zeolites. Larger-pore zeolites could potentially be created via fluoride-mediated syntheses<sup>22,23</sup>, but the presence of a strong acid like hydrofluoric acid would cause decomposition of the photolabile molecule, since it is also acid-cleavable. Lastly, the formation of the zeolite MFI in some of the syntheses could also be due to the presence of contaminants in the Teflon liners used for synthesis, or from some slight degradation of the P-SDA 1 molecules, undetected via NMR, to smaller molecules which could aid the formation of MFI crystals. This suggests that although low-intensity, very small crystals of MFI could be crystallized occasionally, P-SDA 1 does not have the structure-directing capabilities required to demonstrate the feasibility of the photolabile structure-directing agent route to zeolite synthesis.

### 3. Conclusions

Despite the ability of the photolabile molecule P-SDA 1 (8,8-dimethyl-2-(2-nitrophenyl)-1,4-dioxo-8-azoniaspiro[4.5]decane hydroxide) to undergo cleavage while occluded within the pore space of a large-cage zeolite, it has poor structure-directing ability over a range of synthetic conditions intended to produce such zeolite materials as BEA\*, MFI, and MOR. Generally, these syntheses result in amorphous or layered materials after long crystallization times, but occasionally produce small amount of very small crystals of MFI material. These latter syntheses are unfortunately not reproducible. The inability of this molecule to produce a microporous, crystalline material is likely due to a combination of factors, including its large size, bulky aromatic group, and changed electrostatic interaction potential due to the nitro substituent's electron-withdrawing

nature when compared to the acid-cleavable equivalent of P-SDA 1. Although this particular molecule did not demonstrate the feasibility of the photolabile structure-directing agent route to zeolite syntheses, it did demonstrate the ability of the 2-nitrobenzyl class of molecules to cleave within a zeolite pore space when the material is in planar conformation. This suggests that this class of molecules could be useful for this route; future work should therefore focus on the development of smaller photolabile structure-directing agents, potentially with different synthetic conditions, such as the aluminophosphate zeolites, which could yield zeolitic material in shorter crystallization times to prevent degradation caused by exposure to elevated temperatures and caustic conditions over long periods of time.

## **4. Experimental**

### **4.1 Synthesis of P-SDA 1**

The synthesis of P-SDA 1 proceeds as shown in Figure 6.2, with a ketalization reaction followed by quaternization of the secondary amine.

#### **4.1.1 Ketalization Reaction**

4.00 g of 1-(2-nitrophenyl)ethane-1,2-diol (98%, Aldrich), 10.00 g of 4-piperidone monohydrate hydrochloride (98%, Aldrich), and 0.05 g p-toluenesulfonic acid monohydrate (99%, Aldrich) were suspended in 50 mL cyclohexane (EMD) in a round-bottom flask covered with aluminum foil. The suspension was refluxed under an N<sub>2</sub> atmosphere, while any water generated from the reaction was removed using a Dean-Stark apparatus. Yellow solids were produced. The solvent was evaporated using a

rotary evaporator. The solids were then re-suspended in 20 mL chloroform (EMD), and 1 mL of a saturated solution of potassium carbonate (Aldrich) in water was added to the solution to neutralize the p-toluenesulfonic acid. 5 mL water was then added to dissolve the excess 4-piperidone monohydrate hydrochloride. The product, 2-(2-nitrophenyl)-1,4-dioxo-8-azaspiro[4.5]decane, was recovered by extracting the aqueous phase several times with chloroform. The chloroform cuts were combined and evaporated to obtain the pure product in approximately 95% yield. <sup>1</sup>H NMR (dimethyl sulfoxide-d<sub>6</sub>) data for this molecule before amine quaternization indicate peaks at 2.1, 3.1, 3.8, 4.6, 5.6, 7.6, 7.8, 8.1, and 8.3.

#### 4.1.2 Amine Quaternization Reaction

4.15 g of 2-(2-nitrophenyl)-1,4-dioxo-8-azaspiro[4.5]decane (synthesis) and 2.89 g of triethylamine (Aldrich) were added to 30 mL methanol (EMD) in a round-bottom flask covered in aluminum foil while stirring. The round-bottom flask was capped with a rubber septum and placed in an ice bath. The solution was then placed under an Ar atmosphere. 10.15 g of methyl iodide (99.5%, Aldrich) was added drop-wise by injection over a period of 3 minutes. The mixture was stirred for 1 day at room temperature, producing yellow solids after a period of an hour. The solids were separated from the organic solution by centrifugation, and washed several times with diethyl ether (J.T. Baker). The solids were then recrystallized from chloroform (EMD) and diethyl ether to completely remove the triethylamine proton acceptor and to give the product, 8,8-dimethyl-2-(2-nitrophenyl)-1,4-dioxo-8-azoniaspiro[4.5]decane iodide in 50 – 70 % yield. <sup>13</sup>C CPMAS NMR indicated peaks for the pure iodide salt ketal at 148.0, 140.5,

134.7, 130.1, 124.4, 123.3, 104.1, 74.3, 69.5, 60.2, 52.3, 42.9, 30.5, and 25.2. The quaternary ammonium iodide salts, 8,8-dimethyl-2-(2-nitrophenyl)-1,4-dioxaspiro[4.5]decane iodide, were converted to the corresponding hydroxide form in 97.9% yield using Bio-Rad AG1-X8 anion exchange resin.

## 4.2 Photocleavage of P-SDA 1

### 4.2.1 Homogeneous Cleavage of P-SDA 1

0.050 g of P-SDA 1 in its iodide salt form was dissolved in 2.5 mL of solvent (water, acetonitrile (EMD), N,N-dimethylformamide (EMD), dimethylsulfoxide (EMD), and benzene (EMD)), and placed in a quartz tube under stirring and Ar. A long-wave UV lamp (UVP Model B 100 AP) was positioned such that the lamp head was directed towards the side of the tube, and the head and the area surrounding the sample were enclosed with aluminum foil for safety reasons. The sample was irradiated for up to 24 h with UV radiation of wavelength 320 nm or greater UV lamp (UVP Model B 100 AP). After irradiation, the sample was investigated with either  $^1\text{H}$  NMR, Electrospray Ionization Mass Spectrometry (MassSpec), or Infrared Radiation Spectrometry (IR).

### 4.2.2 Photocleavage of P-SDA 1 Intercalated within Tosoh 390-HUA, a Dealuminated Zeolite X (Structure Code FAU)

0.300 g of Tosoh 390-HUA dealuminated zeolite X (structure code FAU) were activated to remove any water or organic materials accumulated within the pore space by heating, while under vacuum, the sample in a sealed quartz tube equipped with a stirbar at 140 °C for 12 h. The sample was then allowed to cool under vacuum, and then removed from

vacuum, maintaining a small ( $2 \times 10^{-5}$  Torr) vacuum in the quartz tube. A solution of 0.020 g of P-SDA 1 in its iodide salt form in 0.8 mL acetonitrile was then slowly injected into the quartz tube, while stirring, and stirring the resulting mixture for 24 h. The solvent was then evaporated under argon flow, and the sample was dried to  $2 \times 10^{-5}$  Torr.<sup>24</sup> Solid-state  $^{13}\text{C}$  cross-polarization magic-angle spinning nuclear magnetic resonance (CPMAS NMR) and TGA were carried out on both the solid P-SDA 1 iodide salt (prior to intercalation) and the FAU sample (post-intercalation) to determine the success of the procedure. The mixture was then slurried into 3 mL of water, sonicated to disperse the suspended particles, and drop-coated onto glass slides bounded with clear sticky tape to constrain the sample to a  $2 \times 2 \text{ cm}^2$  area on the slides. The slides were then dried at room temperature for 12 h to form a thin layer of zeolite and P-SDA 1 (iodide form) on the surface of the slides, and then placed in a glass petri dish for photolysis experiments. A long-wave UV lamp (UVP Model B 100 AP) was positioned such that the lamp head was directed above the layer, and the head and the area surrounding the sample were enclosed with aluminum foil for safety reasons. The sample was irradiated for up to 24 h with UV radiation of wavelength 320 nm or greater UV lamp (UVP Model B 100 AP). After irradiation, the P-SDA 1 fragments were extracted from the layer by scraping the layer off the slide, then washing with acetonitrile to separate the P-SDA 1 fragments from the zeolite. The organic solvent was removed, and the remaining fragments of P-SDA 1 were identified with either  $^1\text{H}$  NMR, MassSpec, or IR techniques.

### 4.3 Zeolite Synthesis with P-SDA 1

Silicate and aluminosilicate zeolite syntheses were attempted using P-SDA 1 as the structure-directing agent. The syntheses attempted (Table 6.1) were based on standard syntheses to produce silicate or aluminosilicate zeolites BEA\* and MFI, and used the following general procedures. First, the sources of the charge-balancing cations and mineralizing agent were completely dissolved in distilled, de-ionized water in a small Teflon jar equipped with a screw-on lid and a stirbar. The alumina source (if required) was then dissolved in the solution while stirring for 30 – 75 min. An aqueous solution of P-SDA 1 was then added according to the required gel composition, and stirred for 10 – 30 min. The silica source (usually Cab-O-Sil fumed silica, Ludox colloidal silica, or tetraethylorthosilicate (Aldrich)) was then slowly added, and the solution was stirred for up to 16 h to ensure homogeneity. In some cases, calcined, previously prepared zeolite seeds were added (up to 5 wt % of the silica source) to the gel to encourage crystallization. The zeolite gel was then transferred into a Teflon-lined Parr Autoclave, which was placed in an oven and crystallized at 150 °C or 165 °C until phase separation occurred. In some cases, the autoclave was placed on a rotating spit inside the oven to decrease the crystallization time required. If, after 60 days, phase separation did not occur, the reaction was stopped. After removal from the oven, the solid material was collected from the autoclave by filtration and centrifugation, and washed exhaustively with water and acetone. The sample was then dried overnight in a 100 °C oven.

All of the attempted zeolite syntheses shown in Table 6.1 were not only run in duplicate, but also run without the SDA, and with 1,1-dimethyl-4-oxopiperidinium hydroxide (the

fragment resulting from photolytic cleavage of P-SDA 1) as controls to verify that a zeolite material could not crystallize unless the P-SDA 1 was intact. All the samples were characterized using X-ray diffraction (XRD), Thermogravimetric Analysis (TGA), and  $^{13}\text{C}$  CP/MAS NMR to verify crystallization and that the P-SDA 1 molecule was intact. If the molecule was intact, it was then cleaved using the procedures outlined above for the P-SDA 1 intercalated into Tosoh 390-HUA.

#### 4.4 Characterization

The materials were characterized using a combination of liquid-state  $^1\text{H}$  and solid-state  $^{13}\text{C}$  nuclear magnetic resonance (NMR), infrared spectroscopy (IR), thermogravimetric analysis (TGA), and powder X-ray diffraction (XRD). NMR analysis was carried out with a Varian Mercury 300 MHz spectrometer (liquid state) and a Bruker AM 300 MHz spectrometer (solid-state). IR analysis was carried out on a Nicolet Nexus 470 FTIR spectrometer. TGA was performed on a NETZSH STA 449C analyzer in air using an aluminum sample pan. XRD was carried out on a Scintag XDS 2000 diffractometer operated at -45 kV and 40 mA using  $\text{Cu K}_\alpha$  radiation ( $\lambda = 1.54056 \text{ \AA}$ ) in the  $2\theta$  range of 2-40 at a step size of  $0.5^\circ / \text{min}$ .

## 5. References

- <sup>1</sup> Lee, H., Zones, S. I. & Davis, M. E. A combustion-free methodology for synthesizing zeolites and zeolite-like materials. *Nature* **425**, 385-388 (2003).
- <sup>2</sup> Lee, H., Zones, S. I. & Davis, M. E. Synthesis of molecular sieves using ketal structure-directing agents and their degradation inside the pore space. *Microporous Mesoporous Mat.* **88**, 266-274 (2006).
- <sup>3</sup> Dong, J. H., Lin, Y. S., Hu, M. Z. C., Peascoe, R. A. & Payzant, E. A. Template-removal-associated microstructural development of porous-ceramic-supported MFI zeolite membranes. *Microporous Mesoporous Mat.* **34**, 241-253 (2000).
- <sup>4</sup> Tosheva, L. & Valtchev, V. P. Nanozeolites: Synthesis, crystallization mechanism, and applications. *Chem. Mater.* **17**, 2494-2513 (2005).
- <sup>5</sup> Wang, H. T., Wang, Z. B. & Yan, Y. S. Colloidal suspensions of template-removed zeolite nanocrystals. *Phys. Chem. Chem. Phys.* **2**, 2333-2334 (2000).
- <sup>6</sup> Smaïhi, M., Gavilan, E., Durand, J. O. & Valtchev, V. P. Colloidal functionalized calcined zeolite nanocrystals. *J. Mater. Chem.* **14**, 1347-1351 (2004).
- <sup>7</sup> Gautier, B. & Smaïhi, M. Template extraction from surface-functionalised zeolite beta nanoparticles. *New J. Chem.* **28**, 457-461 (2004).
- <sup>8</sup> Boudreau, L. C. & Tsapatsis, M. A highly oriented thin film of zeolite A. *Chem. Mater.* **9**, 1705 (1997).
- <sup>9</sup> Valtchev, V. & Mintova, S. Layer-by-layer preparation of zeolite coatings of nanosized crystals. *Microporous Mesoporous Mat.* **43**, 41-49 (2001).

- <sup>10</sup> Liu, Y., Zhang, W. Z. & Pinnavaia, T. J. Steam-stable aluminosilicate mesostructures assembled from zeolite type Y seeds. *J. Am. Chem. Soc.* **122**, 8791-8792, doi:10.1021/ja001615z (2000).
- <sup>11</sup> Platas-Iglesias, C. *et al.* Zeolite GdNaY nanoparticles with very high relaxivity for application as contrast agents in magnetic resonance imaging. *Chem.-Eur. J.* **8**, 5121-5131 (2002).
- <sup>12</sup> Mintova, S. & Bein, T. Nanosized zeolite films for vapor-sensing applications. *Microporous Mesoporous Mat.* **50**, 159-166 (2001).
- <sup>13</sup> Pillai, V. N. R. Photoremovable Protecting Groups in Organic Synthesis. *Synthesis* **1980**, 1-27 (1980).
- <sup>14</sup> Guss, C. O. The Reactions Of Meta-Nitrostyrene And Ortho-Nitrostyrene Oxide With Phenol. *J. Org. Chem.* **17**, 678-684 (1952).
- <sup>15</sup> Gravel, D., Hebert, J. & Thoraval, D. Ortho-Nitrophenylethylene Glycol As Photoremovable Protective Group For Aldehydes And Ketones - Syntheses, Scope, And Limitations. *Can. J. Chem.-Rev. Can. Chim.* **61**, 400-410 (1983).
- <sup>16</sup> Gravel, D., Giasson, R., Blanchet, D., Yip, R. W. & Sharma, D. K. Photochemistry Of The Ortho-Nitrobenzyl System In Solution - Effects Of O-H Distance And Geometrical Constraint On The Hydrogen Transfer Mechanism In The Excited-State. *Can. J. Chem.-Rev. Can. Chim.* **69**, 1193-1200 (1991).
- <sup>17</sup> Bein, T. Synthesis and applications of molecular sieve layers and membranes. *Chem. Mater.* **8**, 1636-1653 (1996).

- 18 Lew, C. M., Li, Z. J., Zones, S. I., Sun, M. W. & Yan, Y. S. Control of size and yield of pure-silica-zeolite MFI nanocrystals by addition of methylene blue to the synthesis solution. *Microporous Mesoporous Mat.* **105**, 10-14 (2007).
- 19 Li, S. A., Li, Z. J. & Yan, Y. S. Ultra-low-k pure-silica zeolite MFI films using cyclodextrin as porogen. *Adv. Mater.* **15**, 1528 (2003).
- 20 Lee, H., Zones, S. I. & Davis, M. E. in *Recent Advances In The Science And Technology Of Zeolites And Related Materials, Pts A - C* Vol. 154 *Studies In Surface Science And Catalysis* 102-109 (2004).
- 21 Flanigen, E. M. *et al.* Silicalite, A New Hydrophobic Crystalline Silica Molecular-Sieve. *Nature* **271**, 512-516 (1978).
- 22 Corma, A., Rey, F., Rius, J., Sabater, M. J. & Valencia, S. Supramolecular self-assembled molecules as organic directing agent for synthesis of zeolites. *Nature* **431**, 287-290 (2004).
- 23 Caullet, P., Paillaud, J. L., Simon-Masseron, A., Soulard, M. & Patarin, J. The fluoride route: a strategy to crystalline porous materials. *Comptes Rendus Chimie* **8**, 245-266 (2005).
- 24 Turro, N. J., Lei, X. G., Li, W., Liu, Z. Q. & Ottaviani, M. F. Adsorption of cyclic ketones on the external and internal surfaces of a faujasite zeolite (CaX). A solid-state H-2 NMR, C-13 NMR, FT-IR, and EPR investigation. *J. Am. Chem. Soc.* **122**, 12571-12581 (2000).